Pergamon

Int. J. Solids Structures Vol. 33, No. 28, pp. 4131–4142, 1996

0020-7683/96 $15.00 + .00

0020-7683(95)00245-6

EFFECTS OF THERMOELASTICITY AND A VON MISES CONDITION IN RAPID STEADY-STATE QUASI-BRITTLE FRACTURE

L. M. BROCK
Engineering Mechanics, University of Kentucky, Lexington, Kentucky 40506, U.S.A.

(*Received* 27 *February* 1995; *in revised form* 27 *September* 1995)

Abstract—Rapid steady-state crack growth in a coupled thermoelastic solid at room temperature is considered. The process is quasi-brittle in the sense that a Dugdale inelastic zone forms ahead of the crack. However, the yield condition defining the zone is of the multiaxial von Mises type, which introduces a non-linear condition into the analysis. This zone also acts as an effective heat source for the surrounding thermoelastic material. The zone heat flux function is not known initially, however, but is treated as a process parameter.

The associated mixed boundary value problem is solved by a Wiener-Hopf technique, and experimentally-based values for the crack speed and near-crack temperature rise then imposed. This calibration process allows comparisons of the model with standard Dugdale models in non-thermal solids to be made without having to impose a complete fracture criterion.

Results show that coupled thermoelasticity and the von Mises condition enhance both inelastic zone size and dynamic fracture toughness, and that this effect increases with crack speed. The zone length values also show agreement with experimentally-based calculations. Copyright © 1996 Published by Elsevier Science Ltd.

INTRODUCTION

Experimental results (Zehnder and Rosakis, 1991; Mason and Rosakis, 1992; Kallivayalil and Zehnder, 1994) indicate that significant temperature rises can occur under room-temperature conditions in rapid dynamic fracture due to crack edge plasticity. In studying this process, a standard approach (e.g. Weichert and Schoenert, 1978) is to model the heat production as a plastic work term in the thermal diffusion equation. This model simplifies mathematics by neglecting thermoelastic coupling (Boley and Weiner, 1960; Chadwick, 1960) and can be justified by analysis (Freund and Hutchinson, 1985) and by the concentrated nature of the crack edge plastic zone. Indeed, Rice and Levy (1969) employed the Dugdale (1960) vanishing-thin yield zone model, a practice perhaps validated by Mason and Rosakis (1992), who calculated from measured temperatures that the plastic zone length in the crack plane can be several times its transverse dimension.

In view of this zone geometry, Brock *et al.* (1992), Brock and Thomas (1992) and Brock (1993) took a somewhat different approach: the Dugdale (1960) model was adopted, but its heat production, as well as its related plasticity, were treated as boundary effects for a surrounding coupled thermoelastic solid. Similar models had been used for non-dynamic fracture (Parvin, 1979), but the heat-production properties of the zone were assumed; here, they were determined from the analysis. This approach does not require the specific details of thermoplasticity, yet can incorporate experimental data in what might be called an effective model of thermally-sensitive dynamic fracture.

In particular, inelastic crack edge temperature fields (Mason and Rosakis, 1992) were used by Brock (1994) in an idealized 2D model of rapid steady-state crack growth. Results showed that thermal coupling parameters do influence plastic zone size and the relation between applied load and crack speed. However, two important issues were not addressed—fracture toughness and multiaxiality in imposing zone yield criteria.

The former is, of course, a key parameter in fracture mechanics (Ewalds and Wanhill, 1985) and is known to be sensitive to temperature (Zehnder and Rosakis, 1991). The latter issue arises because, in the standard Dugdale (1960) model, yield occurs when some component of normal stress reaches a critical value. However, Becker and Gross (1988)

showed for non-thermal equilibrium cracks that, under multiaxial loading, this model gives results that differ from those arising from a zone governed by a true von Mises (Hill, 1950) multiaxial yield criterion. Even more recently, Brock (1995a) showed that, for dynamic fracture, even pure tension loading under a von Mises condition gives results different from those due to the standard Dugdale model.

In this study, therefore, the work of Brock (1994) is extended to include a Dugdale zone that satisfies a von Mises relation, and to consider the effects of coupled thermoelasticity on fracture toughness. Because the relation is non-linear, the possibility of non-uniqueness arises. However, it will be seen that solution candidates can be constructed, and a single solution chosen on the basis of one equation.

As with Brock's (1994) work, an unbounded linearly thermoelastic isotropic, homogeneous sheet is treated. A semi-infinite crack is opened in the sheet by equal compressive point forces (line loads across the sheet thickness) which move along the two crack faces. The process is assumed to reach a steady-state in which the crack edge and forces move at the same constant, subcritical speed, and the Dugdale (1960) zone maintains a constant length. The crack propagation satisfies a COD criterion (Ewalds and Wanhill, 1985) although, as with Brock's (1994) results, some of the conclusions drawn do not depend explicitly on a criterion.

In the next section, the problem is formulated and solved. The fracture toughness is then studied, along with other solution aspects. Comparisons are made with a corresponding non-thermal analysis and with the standard (non-thermal) Dugdale (1960) model. In another contrast with the work of Brock (1994), this analysis will make use of expressions that are valid near the inelastic zone edge yet, at the same time, give a temperature formula that relies less on approximate forms.

PROBLEM FORMULATION

Consider the unbounded xy-plane occupied by a thermoelastic sheet, at rest at a uniform room temperature $T_o(K)$. A semi-infinite crack grows along the x-axis, driven by two equal compressive moving forces (line loads in the out-of-plane direction) of magnitude P. An inelastic zone of length d and vanishing thickness forms ahead of the crack, and the process is shown in Fig. 1 after a steady-state situation has been achieved. In Fig. 1, the two forces remain a fixed distance $L \geqslant d$ behind the inelastic zone edge and all three items—force pair, crack and inelastic zone—propagate at a constant, subcritical speed. Here c is that speed non-dimensionalized with respect to the classical dilatational wave speed (Achenbach, 1973) v_1 in the corresponding non-thermal solid. Its subcritical nature requires that

$$c < c_o \tag{1}$$

where c_o will be discussed in the course of the analysis.

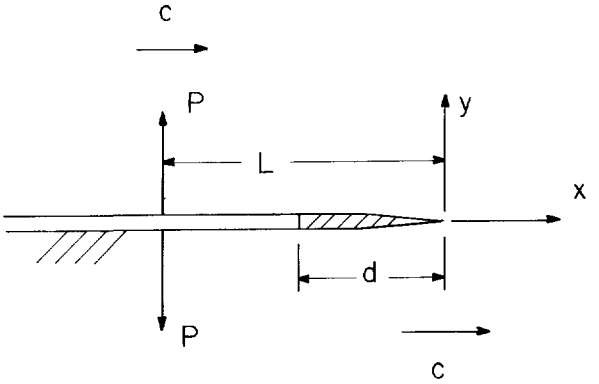

Fig. 1. Force-driven rapid quasi-brittle fracture process.

Problem symmetry can be invoked to reduce consideration to the half-plane $y > 0$. There, the governing steady-state equations for this process are

$$\nabla^2\mathbf{u}+\nabla[(m^2-1)\Delta+\kappa\omega]-m^2c^2\mathbf{u}''=0,\kappa=\kappa_o(4-3m^2),m=\frac{v_1}{v_2} \tag{2a}$$

$$\frac{k}{\mu}\nabla^2\omega+c_h\frac{m}{v_2}c\omega'-c\kappa T_o\Delta'=0 \tag{2b}$$

$$\frac{1}{\mu}\boldsymbol{\sigma}=[(m^2-2)\Delta+\kappa\omega]\mathbf{I}+\nabla\mathbf{u}+\mathbf{u}\nabla \tag{2c}$$

where $\mathbf{u}(x,y)$ is the 2D displacement vector with components (u_x,u_y), $\omega(x,y)$ is the change in temperature from T_o, $(\ )'$ denotes x-differentiation, Δ is the dilatation and $\boldsymbol{\sigma}(x,y)$ is the plane stress tensor. As seen in Fig. 1, the coordinates (x,y) move with the inelastic zone edge. The constants (κ_o,v_2,k,μ,c_h) are, respectively, the coefficient of thermal expansion, rotational wave speed, thermal conductivity, shear modulus and specific heat.

Equations (2) follows from the general equations for an isotropic, homogeneous thermoelastic solid presented by Chadwick (1960) and Boley and Weiner (1960). In a more exact form, the last term in (2b) would involve the product of the dilatation rate and the instantaneous, as opposed to the initial, value of the absolute temperature. As noted by Chadwick (1960), use of the initial value T_o can be justified if the instantaneous and initial values are close but that, in any case, its use allows a useful approximation to what would otherwise be a non-linear set of equations.

The boundary conditions along $y=0$ are

$$\sigma_{xy}=0 \tag{3}$$

for all x and

$$\partial\omega=0(x<-d,x>0),\partial\omega=F(x)(-d<x<0) \tag{4a}$$

$$\sigma_y=-P\delta(x+L)(x<-d),u_y=0(x>0) \tag{4b}$$

while for $-d<x<0$ the von Mises relation

$$(\sigma_x-\sigma_y)^2+\sigma_x^2+\sigma_y^2=2Y^2 \tag{5}$$

for plane stress holds. Here δ is the Dirac function, Y is the yield stress measured in simple tension at T_o and ∂ denotes y-differentiation. The function $F(x)$ is the effective heat flux associated with the inelastic zone, and must be found in the course of the analysis. For now, we assume that it is finite and continuous for $-d<x<0$. In addition, we require that $(\mathbf{u},\omega)$ be bounded for $\sqrt{(x^2+y^2)}\to\infty$ and continous for $y>0$.

To solve this system, we temporarily relax (5) and replace the mixed condition (4b) with the unmixed set

$$\sigma_y=-P\delta(x+L)(X<-d),\sigma_y=\sigma(x)(-d<x<0),\sigma_y=\Sigma_+(x)(x>0) \tag{6a}$$

$$2u_y=U_-(x)(x<0),u_y=0(x>0) \tag{6b}$$

Here σ is the unknown normal stress on the inelastic zone, Σ_+ is the unknown normal stress ahead of the zone and U_- is the unknown crack/inelastic zone separation. Continuity of $\mathbf{u}$ for $y>0$ requires that

$$U_-(0^-)=0 \tag{7}$$

If σ is treated as if is were known, then the relaxed problems (2), (3), (4a) and (6) can be

solved and the unknown functions (Σ_+, U_-) obtained by use of the Wiener-Hopf technique (Noble, 1958). This process is outlined in the next section.

RELAXED PROBLEM SOLUTION TRANSFORMS

Application of the bilateral Laplace transform (Sneddon, 1972)

$$g^* = \int_{-\infty}^{\infty} g\, \mathrm{e}^{-qx}\, \mathrm{d}x \tag{8}$$

to (2), where q is generally complex, gives the transform solutions

$$\begin{bmatrix} \dfrac{\kappa}{m^2}\omega^* \\ u_x^* \\ u_y^* \end{bmatrix} = \begin{bmatrix} 1 & 1 & 0 \\ -q & -q & \beta \\ \alpha_+ & \alpha_- & q \end{bmatrix} \begin{bmatrix} A_+ \mathrm{e}^{-\alpha_+ y} \\ A_- \mathrm{e}^{-\alpha_- y} \\ B\mathrm{e}^{-\beta y} \end{bmatrix} \tag{9a}$$

$$\frac{1}{\mu}\begin{bmatrix} \sigma_{xy}^* \\ \sigma_x^* \\ \sigma_y^* \end{bmatrix} = \begin{bmatrix} 2q\alpha_+ & 2q\alpha_- & -T \\ T_+ & T_- & 2q\beta \\ -T & -T & -2q\beta \end{bmatrix} \begin{bmatrix} A_+ \mathrm{e}^{-\alpha_+ y} \\ A_- \mathrm{e}^{-\alpha_- y} \\ B\mathrm{e}^{-\beta y} \end{bmatrix} \tag{9b}$$

In (9), (A_+, B) are arbitrary functions of q while

$$\alpha_\pm = \sqrt{-qc}\sqrt{(\rho_+ \pm \rho_-)^2 + \frac{q}{c}}, \beta = b\sqrt{-q^2} \tag{10a}$$

$$T = q^2 K, T_\pm = 2\alpha_\pm^2 - m^2 c^2 q^2 \tag{10b}$$

$$M_\pm = -qc[qc + (\rho_+ \pm \rho_-)^2], \quad 4\rho_\pm^2 = \left(\sqrt{-qc} \pm \frac{1}{\sqrt{h}}\right)^2 + \frac{\varepsilon}{h} \tag{10c}$$

$$b = \sqrt{1 - m^2 c^2}, \quad K = m^2 c^2 - 2, \quad h = \frac{k v_2}{\mu c_h m}, \quad \varepsilon = \frac{T_o}{c_h}\left(\frac{v_2 \kappa}{m}\right)^2 \tag{10d}$$

For boundedness in $y > 0$, we set $\mathrm{Re}(\alpha_-, \beta) \geqslant 0$ in the planes cut along $\mathrm{Im}(q) = 0$ and $|\mathrm{Re}(q)| > 0$, while $\mathrm{Re}(\alpha_-) \geqslant 0$ in the plane cut along $\mathrm{Im}(q) = 0$, $\mathrm{Re}(q) < -c[1 + \varepsilon/(1 - c^2)]/h$. In (10d), the dimensionless parameter ε is the thermal coupling constant, and generally (Chadwick, 1960) has values of order $O(10^{-2})$, while h is a thermoelastic characteristic length, with values generally (Brock, 1992) of order $O(10^{-3})\mu$m. In some calculations, the alternative expressions

$$M_\pm = -qc(\bar{\rho}_+ \pm \bar{\rho}_-)^2, \quad 4\bar{\rho}_\pm^2 = \left(\sqrt{qc} \pm \sqrt{\frac{\varepsilon}{h}}\right)^2 + \frac{1}{h} \tag{11}$$

to (10c) prove useful. Application of (8) to (3), (4a) and (6a) gives a set of three conditions along $y = 0$ that, upon substitution of (9), can be solved for (A_+, B):

$$D\begin{bmatrix} \pm A_{\pm} \\ \dfrac{1}{2q}B \end{bmatrix} = \begin{bmatrix} -M_{\pm}R_{\mp} & \dfrac{\varepsilon}{h}\alpha_{\pm}T(qc)^3 \\ T(\alpha_- - \alpha_+) & \alpha_+\alpha_-(M_- - M_+) \end{bmatrix} \begin{bmatrix} \dfrac{\kappa}{m^2}\int_{-d}^{0} F\mathrm{e}^{-qt}\,\mathrm{d}t \\ \dfrac{1}{\mu}\int_{-d}^{0}\sigma\mathrm{e}^{-qt}\,\mathrm{d}t + \dfrac{1}{\mu}\Sigma_+^* - \dfrac{P}{\mu}\mathrm{e}^{qL} \end{bmatrix} \tag{12a}$$

$$D = R_-(M\alpha)_+ - R_+(M\alpha)_-, \quad R_{\pm} = 4q^2\beta\alpha_{\pm} + T^2 \tag{12b}$$

Operation of (8) on (6b) gives in view of (9a) and (12) the Wiener-Hopf equation

$$2\frac{m^2c^2q^2}{D}(\alpha_- - \alpha_+)\left[\frac{\kappa T}{m^2}\int_{-d}^{0} F\mathrm{e}^{-qt}\,\mathrm{d}t + \frac{\alpha_+\alpha_-}{\mu}(\alpha_- + \alpha_+)\left(\int_{-d}^{0}\sigma\mathrm{e}^{-qt}\,\mathrm{d}t + \Sigma_+^* - P\mathrm{e}^{qL}\right)\right] = U_{\pm}^* \tag{13}$$

As discussed earlier, the solution obtained here need be valid only for small $|x|$. In view of the Tauberian theorems, therefore, transforms valid for large $|q|$ can be used, and the asymptotic results

$$\alpha_+ = a\sqrt{-q^2}, M_+ = 0, R_+ = -q^4R \tag{14a}$$

$$\alpha_- = \sqrt{q}\sqrt{q+\lambda}, M_- = -q\lambda, R_- = q^3[qK^2 - 4b\sqrt{q}\sqrt{q+\lambda}] \tag{14b}$$

extracted from (10), where

$$R = 4ab - K^2, a = \sqrt{1-c^2}, \lambda = c\frac{\varepsilon}{h} \tag{14c}$$

Here R is the classical Rayleigh function (Achenbach, 1973), with zeroes at $q = (0, \pm c_o)$, where (Brock, 1992)

$$m^2c_o = \sqrt{2(m^2-1)}G_o, \quad \ln G_o = -\frac{1}{\pi}\int_1^m \tan^{-1}\frac{4t^2\sqrt{t^2-1}\sqrt{m^2-t^2}}{(m^2-2t^2)^2}\frac{\mathrm{d}t}{t} \tag{15}$$

The term v_1c_o is the non-thermal Rayleigh wave speed, and we will take the c_o in (1) to be defined by (15). Equation (13) then takes the simpler form

$$\frac{\kappa Kc^2}{\lambda R\sqrt{-q}}\left(1 - \frac{a\sqrt{q}}{\sqrt{q+\lambda}}\right)\int_{-d}^{0} F\mathrm{e}^{-qt}\,\mathrm{d}t - \frac{m^2c^2a}{\mu R\sqrt{q}}\left(\int_{-d}^{0}\sigma\mathrm{e}^{-qt}\,\mathrm{d}t + \Sigma_+^* - P\mathrm{e}^{qL}\right) = \frac{\sqrt{-q}}{2}U_{\pm}^* \tag{16}$$

The U-term and the first F-terms in (16) are analytic for $\mathrm{Re}(q) < 0+$, while the Σ-term is analytic for $\mathrm{Re}(q) > 0-$. By following procedures outlined by Noble (1958), the remaining terms in (16) can each be split into two parts, each of which is analytic in an overlapping region of the q-plane. Indeed, the overlapping regions for each pair include the $\mathrm{Im}(q)$-axis. Equation (16) can then be rearranged so that Σ_+^* and all term parts analytic for $\mathrm{Re}(q) > 0-$ are on one side of the equation, while $U_{\pm}^*$ and all term parts analytic for $\mathrm{Re}(q) < 0+$ are on the other. Both sides of the equation must then be considered analytic continuations of the same entire function. The continuity condition (7) and the Tauberian theorems require that $U_{\pm}^*$ behave no worse than $O(q^{-1-\delta})$, $\delta > 0$ as $|q| \to \infty$, so that the U-term in the rearrangement of (16) must vanish as $|q| \to \infty$. Indeed, it can be shown that all the terms analytic for $\mathrm{Re}(q) < 0+$ vanish as $|q| \to \infty$. Liouville's theorem requires, then, that the

aforementioned entire function vanish identically, and the sides of the rearranged (16) can be solved separately for Σ_+^* and U_-^* :

$$\frac{1}{\mu\sqrt{q}}\Sigma_+^* = \frac{1}{\pi\mu}\int_0^\infty \left(P\,\mathrm{e}^{-zL} - \int_{-d}^0 \sigma\,\mathrm{e}^{zt}\,\mathrm{d}t\right)\frac{\mathrm{d}z}{(z+q)\sqrt{z}} + \frac{\kappa K}{m^2\lambda\pi}\int_0^\lambda \frac{\mathrm{e}^{zt}\,\mathrm{d}z}{(z+q)\sqrt{\lambda-z}}\int_{-d}^0 F\,\mathrm{d}t \tag{17a}$$

$$\sqrt{-q}U_-^* = \frac{\kappa c^2 K}{\lambda R}\int_{-d}^0 F\,\mathrm{d}t\left[\frac{\mathrm{e}^{-qt}}{\sqrt{-q}}\left(1-\frac{a\sqrt{q}}{\sqrt{q+\lambda}}\right) - \frac{a}{\pi}\int_0^\lambda \frac{\mathrm{e}^{zt}\,\mathrm{d}z}{(z+q)\sqrt{\lambda-z}}\right]$$
$$-\frac{m^2c^2a}{\mu R}\left[\int_{-d}^0 \sigma\,\mathrm{d}t\left(\frac{\mathrm{e}^{-qt}}{\sqrt{q}} - \frac{1}{\pi}\int_0^\infty \frac{\mathrm{e}^{zt}\,\mathrm{d}z}{(z+q)\sqrt{z}}\right) - P\left(\frac{\mathrm{e}^{qL}}{\sqrt{q}} - \frac{1}{\pi}\int_0^\infty \frac{\mathrm{e}^{-zL}\,\mathrm{d}z}{(z+q)\sqrt{z}}\right)\right] \tag{17b}$$

For $|q|\to\infty$ (17a) gives the asymptotic result

$$\Sigma_+^* \approx \frac{1}{\sqrt{q}}K_I \tag{18a}$$

$$\frac{1}{\mu}K_I = \frac{P}{\mu}\sqrt{\frac{\pi}{L}} - \int_{-d}^0 \frac{\sigma}{\mu}\sqrt{\frac{-\pi}{t}}\,\mathrm{d}t + \frac{\kappa K}{m^2\lambda}\int_{-d}^0 F\,\mathrm{d}t\int_0^\lambda \frac{\mathrm{e}^{zt}\,\mathrm{d}z}{\lambda-z} \tag{18b}$$

The inverse of the function $1/\sqrt{q}$ can be obtained by inspection (Sneddon, 1972) as $1/\sqrt{\pi x}$, $x>0$. That is, the crack plane normal traction Σ_+ exhibits a square-root singularity at the leading edge of the inelastic zone. The Dugdale (1960) model precludes such a singularity, and so

$$K_I = 0 \tag{19}$$

whereupon (17) can be modified to yield

$$\frac{\sqrt{q}}{\mu}\Sigma_+^* = \frac{-1}{\pi\mu}\int_0^\infty \frac{\sqrt{z}\,\mathrm{d}z}{z+q}\left(P\,\mathrm{e}^{-zL} - \int_{-d}^0 \sigma\,\mathrm{e}^{zt}\,\mathrm{d}t\right) - \frac{\kappa K}{m^2\lambda\pi}\int_0^\lambda \frac{\mathrm{e}^{zt}z\,\mathrm{d}z}{(z+q)\sqrt{\lambda-z}}\int_{-d}^0 F\,\mathrm{d}t \tag{20a}$$

$$\sqrt{-q}U_-^* = \frac{\kappa c^2 K}{\lambda R}\int_{-d}^0 F\,\mathrm{d}t\left[\frac{\mathrm{e}^{qt}}{\sqrt{-q}}\left(1-\frac{a\sqrt{q}}{\sqrt{q+\lambda}}\right) + \frac{a}{\pi q}\int_0^\lambda \frac{\mathrm{e}^{zt}z\,\mathrm{d}z}{(z+q)\sqrt{\lambda-z}}\right]$$
$$-\frac{m^2c^2a}{\mu R\sqrt{q}}\left[\int_{-d}^0 \sigma\,\mathrm{d}t\left(\mathrm{e}^{-qt} - \frac{1}{\pi\sqrt{q}}\int_0^\infty \frac{\mathrm{e}^{zt}\sqrt{z}\,\mathrm{d}z}{z+q}\right) - P\left(\mathrm{e}^{qL} + \frac{1}{\pi\sqrt{q}}\int_0^\infty \frac{\mathrm{e}^{-zL}\sqrt{z}\,\mathrm{d}z}{z+q}\right)\right] \tag{20b}$$

With (20) at hand, only the transform inversion process remains to give complete solutions to the relaxed problem valid for small $|x|$. For present purposes, however, only expressions for (u_y, σ_x, ω) along $y=0$ are required. The displacement u_y for $y=0$ is governed by U_-, and the transforms (σ_x^*, ω^*) valid for $y=0$, $|q|$ large can be obtained from (9), (12) and (14) as

$$\frac{1}{\mu}\sigma_x^* = \frac{2\kappa c^2(m^2-1)}{m^2\lambda R\sqrt{q}}\int_{-d}^0 F\,\mathrm{e}^{-qt}\left(\frac{1}{\sqrt{q+\lambda}} - \frac{1}{\sqrt{q}}\right)\mathrm{d}t$$
$$-\frac{1}{\mu}\left[1+\frac{c^2K}{R}\left(m^2-1\right)\right]\left(\int_{-d}^0 \sigma\,\mathrm{e}^{-qt}\,\mathrm{d}t + \Sigma_+^* - P\,\mathrm{e}^{qL}\right) \tag{21a}$$

$$\omega^* = \frac{-1}{\sqrt{-q(q+\lambda)}}\int_{-d}^{0} F e^{-qt}\,dt + \frac{\kappa m^2 c^2 K}{\mu R}\left(\frac{a\sqrt{q}}{\sqrt{q+\lambda}} - 1\right)\left(\int_{-d}^{0} \sigma e^{-qt}\,dt + \Sigma_+^* - P e^{qL}\right) \tag{21b}$$

where Σ_+^* is, of course, given by (20a). The inversion processes for these transforms are outlined in the next section.

SOLUTIONS FOR RELAXED PROBLEM

The inverse of (8) is (Sneddon, 1972)

$$g = \frac{1}{2\pi i}\int_{\Gamma} g^* e^{xq}\,dq \tag{22}$$

where Γ is the Bromwich contour. As an illustration of how this equation is applied to (20b) and (21), consider the very first term in (20b). Substitution of this term into (22) gives the expression

$$\frac{\kappa c^2 K}{\lambda R}\int_{-d}^{0} F\,dt \frac{1}{2\pi i}\int_{\Gamma} \frac{e^{q(x-t)}}{-q}\,dq \tag{23}$$

where Γ must lie to the left of the Im(q)-axis. The q-integrand has a pole at $q = 0$, while the exponential term vanishes in the right-hand half of the q-plane when x-$t < 0$, and in the left-hand half when $x - t > 0$. Cauchy residue theory can then be used to show that

$$\frac{1}{2\pi i}\int_{\Gamma} \frac{e^{q(x-t)}}{-q}\,dq = 0(x > t), \quad 1(x < t) \tag{24}$$

whereupon (23) becomes

$$\frac{\kappa c^2 K}{\lambda R}\int_{x}^{0} F\,dt(-d < x < 0), \frac{\kappa c^2 K}{\lambda R}\int_{-d}^{0} F\,dt(x < -d) \tag{25}$$

Similar procedures can be carried out using (22) for all the terms in (20b) and (21); that is, Cauchy theory can be used to calculate the inversion integral (22) by residues or by transforming the integral to contours along which the integration can be carried out or at least put in more tractable form. Specifically, we find for $x < 0$ that

$$2U_- = \frac{\kappa c^2 K}{\lambda R}\int_{\xi}^{0} F\,dt + 2\frac{m^2 c^2 a}{\pi\mu R}\left[\int_{-d}^{0} \sigma \ln\frac{\sqrt{-t}+\sqrt{-x}}{\sqrt{|t-x|}}\,dt + P\ln\frac{\sqrt{L}+\sqrt{-x}}{\sqrt{|L+x|}}\right]$$
$$- \frac{\kappa c^2 K a}{\pi\lambda R}\int_{0}^{\lambda} \frac{dz}{\sqrt{z(\lambda-z)}}\left[\int_{x}^{0} - \int_{-d}^{0} \operatorname{erf}(\sqrt{-zx})\right] F e^{z(t-x)}\,dt \tag{26}$$

where $\xi = x(-d < x < 0)$ and $\xi = -d(x < -d)$. The function U_- appropriately vanishes at $x = 0-$ and gives

$$2U_{-} = \frac{\kappa c^2 K}{\lambda R}\int_{-d}^{0} F\,\mathrm{d}t\left[1-\frac{a}{\pi}\int_{0}^{\lambda}\frac{\mathrm{e}^{z(t+d)}}{\sqrt{z(\lambda-z)}}\operatorname{erfc}(\sqrt{zd})\,\mathrm{d}t\right]$$
$$+2\frac{m^2c^2a}{\pi\mu R}\left[P\ln\frac{\sqrt{L}+\sqrt{d}}{\sqrt{L-d}}-\int_{-d}^{0}\sigma\ln\frac{\sqrt{-t}+\sqrt{d}}{\sqrt{t+d}}\,\mathrm{d}t\right] \tag{27}$$

at $x = d$. Similarly, for $y = 0, -d < x < 0$ it can be shown that

$$\omega = -\frac{1}{p}\int_{d}^{x} F\mathrm{e}^{-\tau}K_o(\tau)\,\mathrm{d}t-\frac{1}{\pi}\int_{x}^{0} F\mathrm{e}^{-\tau}K_o(-\tau)\,\mathrm{d}t-\frac{\kappa m^2c^2K}{\mu R}(1-a)\sigma(x) \tag{28a}$$

$$\frac{1}{\mu}\sigma_x = -\frac{1}{\mu}\left[1+\frac{c^2K}{R}(m^2-1)\right]\sigma(x)+2\frac{\kappa c^2}{m^2\lambda R}(m^2-1)\left[\int_{x}^{0}+\int_{-d}^{x}\mathrm{e}^{-\tau}I_o(\tau)\right]F\,\mathrm{d}t \tag{28b}$$

In (26)–(28), (erf, erfc) are, respectively, the error and complementary error functions, while (I_o, K_o) are, respectively, the modified Bessel and MacDonald functions (Watson, 1966), and

$$\tau = \frac{\lambda}{2}(x-t) \tag{29}$$

With these forms, the original problem governed by a von Mises condition in the inelastic zone can be treated.

SOLUTION FOR ORIGINAL PROBLEM

In order to satisfy the conditions on the original problem, (5) must be addressed. The use of (6a) and (28b) reduces it to a quadratic in the unknown function σ which can be solved to yield.

$$(3+\chi^2)\frac{\sigma}{2\mu} = -\chi G+\sqrt{(3+\chi^2)\left(\frac{Y}{\mu}\right)^2-3G^2} \tag{30}$$

where

$$\chi = 1+2(m^2-1)\frac{c^2K}{R} \tag{31a}$$

$$G = 2(m^2-1)\frac{\kappa c^2}{m^2\lambda R}\left[\int_{x}^{0} F\,\mathrm{d}t+\int_{-d}^{x} F\mathrm{e}^{-\tau}I_o(\tau)\,\mathrm{d}t\right] \tag{31b}$$

The non-uniqueness introduced by the non-linear equation (5) has manifested itself as two solution candidates. The form of (30) has been chosen because it alone reduces to the standard Dugdale (1960) result $\sigma = Y$ for a tension crack when (F, σ_x) are dropped from the analysis.

Equations (30), (27), (28a) and the restriction (19) govern, in view of a COD-based fracture criterion (Ewalds and Wanhill, 1985), the solution to the original problem. As noted earlier, however, the purpose of this study is to discern the effects of coupled thermoelasticity and a multiaxial yield condition on the dynamic fracture process. Therefore, these equations are used with some limit-case counterparts in the next section to study parameter relations in light of experimentally-verifiable data, but without a fracture criterion being fully imposed.

EFFECTS OF THERMAL COUPLING AND VON MISES RELATION

In this section, fracture toughness and inelastic zone size d are considered for three cases:

Case 0: standard non-thermal/Dugdale zone model
Case 1: present thermal/von Mises zone model
Case 2: non-thermal/von Mises zone model

In case 0, the standard Dugdale (1960) yield condition $\sigma_y = Y(y = 0, -d < x < 0)$ is used, while cases (1, 2) employ the von Mises relation (5). Alternatively, cases (0,2) neglect thermal effects while case 1 employs the coupled thermoelastic formulations (2). Cases (0, 2) are, in effect, limit cases of case 1.

Fracture toughness can be viewed (Ewalds and Wanhill, 1985) as being proportional to the square root of the COD. We will take COD here to be the crack opening U_- at the inelastic zone separation point, $x = -d$, and use toughness for purposes of comparison. The ratio r_{10} of toughness for the present study (case 1) and that for the non-thermal/standard Dugdale model (case 0) is

$$r_{10} = \sqrt{\frac{U_1}{U_0}} \tag{32}$$

Here U_1 is given by (27) and the relations (19) and (30) hold with subscripts 1 affixed, while

$$U_0 = \frac{m^2 c^2 a}{\mu \pi R}\left(P_0 \ln \frac{\sqrt{L}+\sqrt{d}}{\sqrt{L-d}} - Yd\right) \tag{33a}$$

corresponds to U_1 and (30) and (19) are replaced by

$$\sigma_0 = Y, P_0 = 2Y\sqrt{Ld} \tag{33b,c}$$

Similarly, the ratio of toughnesses for a non-thermal/von Mises model (case 2) and that for the non-thermal/standard Dugdale model (case 0) is

$$r_{20} = \sqrt{\frac{U_2}{U_0}} \tag{34}$$

where

$$U_2 = \frac{m^2 c^2 a}{\mu \pi R}\left(P_2 \ln \frac{\sqrt{L}+\sqrt{d}}{\sqrt{L-d}} - \frac{2Yd}{\sqrt{3+\chi^2}}\right) \tag{35a}$$

under the constraints

$$\sigma_2 = \frac{2Y}{\sqrt{3+\chi^2}}, P_2 = \frac{4\sqrt{Ld}}{\sqrt{3+\chi^2}} \tag{35b,c}$$

For a given material, a COD criterion model would specify the quantities (U_0, U_1, U_2) to be the same critical value—U_c, say. Then, for the non-thermal cases (0, 2), the outputs (c, d) could be found from (33a, c) and (35a, c), respectively, in terms of U_c and the loading parameters (P, L). Case 1, however, involves an additional unknown, the flux function F, so that another condition is needed.

In order to keep case comparisons somewhat free of particular criteria and critical values, we here follow Brock (1994) and impose experimentally-based values of crack speed

Table 1

	r_{10}	r_{20}	$(d/L)_0$	$(d/L)_1$	$(d/L)_2$	F(K/mm)
$c = 0.1$	1.0054	1.0041	0.09	0.09374	0.091312	−3284
$c = 0.15$	1.0633	1.0176	0.09	0.095696	0.093192	−4110

c and temperature increases ω at the point of material separation (trailing edge of the inelastic zone). Specifically, from the measurements of Mason and Rosakis (1992) on notched-plate crack propagation under tension, the plausible values

$$\omega = 300 \text{ K} \quad (y = 0, x = -d), \quad c = (0.1, 0.15) \tag{36}$$

are chosen for a steel-like material with properties

$$m = 1.94, \quad \varepsilon = 0.00712, \quad \kappa = -7.1(10^{-5})\frac{1}{\text{K}}, \quad h = 8.2(10^{-4})\ \mu\text{m}, \quad \frac{Y}{\mu} = 0.02 \tag{37}$$

The loading parameters are

$$L = 25 \text{ mm}, \quad \frac{P}{\mu} = 0.3 \text{ mm} \tag{38}$$

and, as a first step, we assume that $F =$ constant for $-d < x < 0$. As noted by Brock (1994), one could in principal approximate the function $F(x)$ by matching expressions for $\omega(x, y)$ to measured values. This curve-fitting procedure would require measurements at different locations very near the zone edge, however, and, despite the careful work of Mason and Rosakis (1992), obtaining such data might not always be feasible. In view of (36)–(38), the equations sets (33) and (35) can be solved for the combinations (U_0, d_0) and (U_2, d_2), while the set (19), (27), (28a) and (30) provides (U_1, d_1). In Table 1, the resulting toughness ratios (r_{10}, r_{20}) as well as the F-values for case 1 and the non-dimensionalized zone sizes d/L for each case are listed.

The data given shows that thermal effects and the von Mises relation enhance both dynamic fracture toughness and inelastic zone size. Moreover, these effects increase with crack speed (c).

It should be noted, however, that more pronounced enhancements were seen (Brock, 1995b) for steady-state tearing of a thermoelastic infinite strip of finite width subjected to fixed insulated edge displacements. The same material properties were employed, but a standard Dugdale (1960) yield law governed the inelastic zone. The different nature of the loading and the presence of material boundaries make a direct comparison of Brock's (1995b) results with those in Table 1 problematic.

The F-values listed are negative, indicating heat flow out of the zone, and exhibit high magnitudes. These high values may follow from modeling the zone as a vanishingly-thin strip. They are lower than corresponding values calculated by Brock (1994) using the same temperature-fit process. That work relied, however, on a standard Dugdale (1960) zone model and on an expression for inelastic zone edge temperature change that, in effect, approximated the modified Bessel functions that appear in (28a). While high F-values might seem to limit the applicability of the strip geometry, it was noted at the outset that work by Mason and Rosakis (1992) does indicate zones with lengths in the crack plane that are several times the transverse dimension. Moreover, the d-values given in Table 1 are, in fact, of the same order of magnitude as their calculated zone lengths.

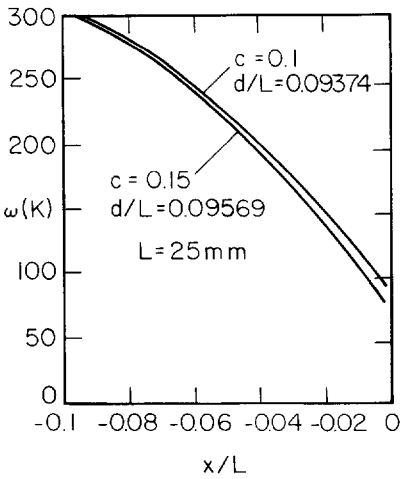

Fig. 2. Variation of temperature along inelastic zone.

TEMPERATURE VARIATION IN THE ZONE

The function F, taken here to a first approximation as a constant, represents heat flux out of the inelastic zone into the surrounding thermoelastic material. The heat flux along the zone may also be of interest, and so in Fig. 2 ω from (28a) is plotted vs $x(-d < x < 0)$ for the combinations listed in Table 1.

Figure 2 shows clearly that the temperature increase is a maximum at the point of material separation and then drops in value as the point of elastic-plastic transition (leading edge of the inelastic zone, $x = y = 0$) is reached. Thus, heat flows from the material separation to the transition point. Granted that this behavior is associated with a particular assumption about F, but the possibility that the point of outright material rupture and maximum extensional strain endures the maximum temperature increase seems plausible. The temperature fields calculated by Mason and Rosakis (1992) show a similar decrease in temperature along the zone length, although their model does, as noted earlier, treat the inelastic-zone-as-heat-source in a standard manner.

BRIEF DISCUSSION

This study considered the rapid, steady-state growth of a crack in an unbounded thermoelastic half-plane driven by moving forces applied to the crack surfaces. The half-plane is initially at rest at a uniform room temperature. A Dugdale (1960) zone represented crack edge inelasticity and, in terms of an effective heat flux function, the heat generated by plastic deformation. The standard uniaxial yield condition in the zone was, however, replaced by a von Mises (Hill, 1950) multiaxial condition.

Despite the presence of an initially unknown flux function, the non-linear condition introduced into the analysis by the von Mises relation, and the coupled nature of the thermoelastic governing equations, analytic solutions valid near the zone edge were obtained from the mixed boundary value problem via the Wiener-Hopf technique.

The Dugdale (1960) zone was assumed to relax any singularities at its leading edge, and a COD criterion was assumed to hold. The non-uniqueness induced by the von Mises relation was removed by choosing that solution that reduced to the standard (non-thermal, uniaxial yield condition) Dugdale model for the running crack.

A critical COD value was not, however, actually imposed. Instead, experimentally-based plausible values for the crack edge temperature increase and crack speed were chosen. The solution behavior, upon comparison, showed that dynamic fracture toughness and zone size are both enhanced by consideration of thermoelastic effects and treatment of a von Mises relation in the zone. The zone lengths found, moreover, were consistent with zone sizes calculated from the same experimentally-determined temperature fields. The enhancement levels actually calculated were small, to be sure, and their increase with crack

speed suggests that more striking results could have been obtained by treating higher speeds. However, a key feature of this work was the study of thermoelastic effects in light of available experimental data, and that data involved the speeds used in calculations.

Calculation also showed that the temperature increase is a maximum at the point of material rupture and, while still significant, decreased along the zone until the elastic-plastic transition point is reached. This suggests that heat flow within the zone is as prominent as the flow out of the zone.

In summary, then, the results here, along with earlier efforts, e.g. Brock (1994), indicate that both thermoelastic considerations and multiaxiality in the yield condition affect the dynamic crack extension process, even at room-temperature conditions.

Acknowledgements—This research was supported by NSF Grant DMS 9121700 and by the NSF/EPSCoR Group in Inverse Problems and QNDE at the University of Kentucky.

REFERENCES

Achenbach, J. D. (1973). *Wave Propagation in Elastic Solids*, North-Holland/American Elsevier, Amsterdam.
Becker, W. and Gross, D. (1988). About the Dugdale crack under mixed mode loading. *Int. J. Fracture* **37,** 163–170.
Boley, B. and Weiner, J. H. (1960). *Theory of Thermal Stresses*, Wiley, New York.
Brock, L. M. (1992). Transient thermal effects in edge dislocation generation near a crack edge. *Int. J. Solids Structures* **29,** 2217–2234.
Brock, L. M. (1993). Early effects of temperature-dependent yield stress in a transient analysis of fracture. *Acta Mechanica* **97,** 101–114.
Brock, L. M. (1994). Coupled thermoelastic effects in rapid steady-state quasi-brittle fracture. *Int. J. Solids Structures* **31,** 1537–1548.
Brock, L. M. (1995a). Wave diffraction-induced crack/cohesive strip growth based on rudimentary non-linear models. *J. Elasticity* **38,** 41–67.
Brock, L. M. (1995b). Rapid quasi-brittle tearing of a thermoelastic strip. *Acta Mechanica* **112,** 95–106.
Brock, L. M., Matic, P. and DeGiorgi, V. G. (1992). Early transient response during crack propagation in a weakly-coupled thermoelastic solid. *Int. J. Solids Structures* **29,** 973–989.
Brock, L. M. and Thomas, J. P. (1992). Thermal effects in rudimentary crack edge inelastic zone growth under stress wave loading. *Acta Mechanica* **93,** 223–239.
Chadwick, P. (1960). Thermoelasticity: the dynamical theory. In *Progress in Solid Mechanics* (eds I. N. Sneddon and R. Hill), North-Holland, Amsterdam.
Dugdale, D. S. (1960). Yielding of steel sheets containing slits. *J. Mech. Physics Solids* **8,** 100–104.
Ewalds, H. L. and Wanhill, R. J. H. (1985). *Fracture Mechanics*, Edward Arnold/Delftse Uitgevers Maatschappij, Delft.
Freund, L. B. and Hutchinson, J. W. (1985). High strain-rate growth in rate-dependent plastic solids. *J. Mech. Physics Solids* **33,** 169–191.
Hill, R. (1950). *The Mathematical Theory of Plasticity*, Clarendon Press, Oxford.
Kallivayalil, J. A. and Zehnder, A. T. (1994). Measurement of the temperature field induced by dynamic crack growth in Beta-C titanium. *Int. J. Fracture* **66,** 99–120.
Mason, J. J. and Rosakis, A. J. (1992). The effects of hyperbolic heat conduction around a dynamically propagating crack. SM Report 92-3, California Institute of Technology, Pasadena, CA.
Noble, B. (1958). *Methods Based on the Wiener-Hopf Technique*, Pergamon Press, New York.
Parvin, M. (1979). Theoretical prediction of temperature rise at the tip of a running crack. *Int. J. Fracture* **15,** 397–404.
Rice, J. R. and Levy, N. (1969). Local heating by plastic deformation at a crack tip. In *Physics of Strength and Plasticity* (ed. A. S. Argon), MIT Press, Cambridge, MA.
Sneddon, I. N. (1972). *The Use of Integral Transforms*, McGraw-Hill, New York.
Watson, G. N. (1966). *A Treatise on the Theory of Bessel Functions*, Cambridge University Press, Cambridge.
Weichert, R. and Schoenert, K. (1978). Heat generation at the tip of a moving crack. *J. Mech. Physics Solids* **26,** 151–161.
Zehnder, A. T. and Rosakis, A. J. (1991). On the temperature distributions at the vicinity of dynamically propagating cracks in 4340 steel. *J. Mech. Physics Solids* **39,** 385–415.